Biomedical Engineering Undergraduate Honors
Theses

Biomedical Engineering

5-2014

# Classification and Quantification of Phenotypic Characteristics of Normal and Dysplastic Oral Cells

Jackson W. Boice
*University of Arkansas, Fayetteville*

Follow this and additional works at: http://scholarworks.uark.edu/bmeguht

Recommended Citation

Boice, Jackson W., "Classification and Quantification of Phenotypic Characteristics of Normal and Dysplastic Oral Cells" (2014).
*Biomedical Engineering Undergraduate Honors Theses*. 4.
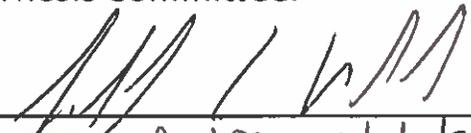http://scholarworks.uark.edu/bmeguht/4

This thesis is approved.
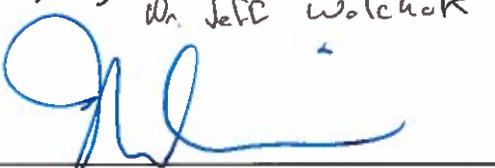
Thesis Advisor:

_Dr. Tim Muldoon_

Thesis Committee:

_Dr. Jeff Wolchok_

_Dah Kim_

Classification and Quantification of Phenotypic Characteristics of Normal and Dysplastic Oral Cells

An Undergraduate Honors College Thesis

in the

Department of Biomedical Engineering
College of Engineering
University of Arkansas
Fayetteville, AR

by

Jackson Wyatt Boice

April 25, 2014

**Summary**

Each year, over 40,000 people acquire oral cancer and over 8,000 deaths are related to oral cancer in the U.S. alone. This equates to about 2.5% of all cancer cases and 1.4% of all cancer related deaths in the U.S. The average five year survival of oral cancer is only 63%, and that statistic drops significantly to under 40% if the cancer is not detected in its early stages. Common screening and diagnostic tools can be physically intimidating to the patient and are time and skill intensive. For those without full access to healthcare, catching a tumor before it becomes deadly is much less common.

This project presents a new method for the harvesting of normal epithelial cells that puts significantly less strain on both the patient and the investigator. Also introduced is a cost effective method for identifying both normal and dysplastic cells using a custom built epi-illuminated LED fluorescent microscope and proflavine as a fluorophore. Using imaging techniques and image analysis tools, the identified cells were analyzed and compared against each other to determine overall patterns of phenotypic expression between normal and dysplastic cells.

The results of analysis indicated a high level of variability between different individual normal oral epithelial cells, and a low level of differentiation amongst cancerous cell types. Normal cells had a low nuclear to cytoplasmic size ratio and a high nuclear to cytoplasmic brightness ratio compared to oral cancer cells, and also presented a much higher entropy in texture overall.

The data presented here can be used as a basis for an index that catalogues the difference between normal and dysplastic cells, and the manual analysis could be converted into an automated process, which would increase the overall ease of use of the screening assay.

**Introduction**

Oral cavity and pharynx cancer account for roughly 2.5% of all new cancer cases in the U.S. per year, with an estimated 42,440 new cases in 2014 [1]. In addition to new cases, there will be approximately 8,000 deaths due to oral and pharyngeal cancer this year in the U.S. alone, accounting for about 1.4%. Oral cancer is one of the cancers with the highest incidence rates, particularly in men. It accounts for roughly sixteen out of every one hundred thousand cases in males, giving it the seventh highest incidence rate within the U.S. [2]. The average five year survival rate of oral cancer is about 63% [3].

Like with most cancers, early detection is the key to high survival rates. Only 30% of all oral cancers are diagnosed in the primary or localized stage of tumor development [1]. When discovered and diagnosed in this stage, the average five year survival rate is high at 82.7%. This drops significantly once the cancer has spread to other parts of the body. The regional survival rate is 60.5% and the distant survival rate is 37.3%. In cases where there was not enough information available to obtain staging information, the five year survival rate was 49.3%.

Even though early detection is the key to survival, not all suspect lesions are given the same investigational treatment. If a mass of tissue is suspected of being malignant, appropriate history of the lesion must be determined, including duration, symptoms, appearance changes, size, color, and texture [4]. If the history indicates possible malignancy, then a biopsy can be ordered. A biopsy is the removal of a sample of tissue from a patient for histopathological examination. Biopsies are the gold standard in tissue diagnoses, and several types of biopsies exist. Incisional biopsies remove a sample of the tissue for examination, while excisional biopsies remove the entire suspect sample. Punch biopsies are similar to incisional biopsies, in that they remove a sample of tissue, but instead of cutting, a punch tool is used, which cuts a

small hole into the tissue. Electrosurgery and laser biopsies are also used, and are useful for large tissues or in cases where closing a wound mechanically would be inappropriate.

Other techniques can be used either separately or to supplement existing biopsy techniques. Brush cytology involves using a cytobrush to vigorously scrub a tissue to remove cells for cytological analysis [5]. Toluidine blue is a dye that stains cell nuclei blue, and because cancer cells have a large nucleus, it can be used to help surgeons identify tumorigenic tissue for removal by staining those legions blue [6].

Although these methods provide extremely accurate results, they are both time and skill intensive, and put unwanted strain on the patient. Because of this, there needs to exist a method for screening that is cost-effective, less time consuming, does not cause physical stress to the patient, and can be performed by investigators with minimal skill. This project proposes an alternative method for the harvesting of normal oral cells using a simple mouthwash technique and combines a cost-effective, custom built epi-illuminated fluorescent microscope system specialized for proflavine fluorescence along with image analysis diagnostic tools as an alternative method for the early screening of possible cancerous tissue of the oral cavity.

Proflavine is an acridine that preferentially stains the nucleus of cells [7] because of the method of interaction it exhibits. Proflavine intercalates between base pairs of DNA [8], causing errors in the genetic data of the cell. . As a fluorophore, it has an excitation peak at 455 nm and an emission peak at 515 nm [9], meaning that when it is illuminated by blue light, it emits a green light. Proflavine has a relatively high quantum efficiency at .34, meaning that even at low energy, excitation light will create a very bright emission spectra [10].

Proflavine was chosen as an experimental fluorophore because it has the ability to stain the nucleus brightly and is much more cost-effective than other fluorescent molecules. In

addition to this, proflavine has no special labelling protocol or incubation time, so it can be used with very little prior knowledge or skill, making it an excellent choice in this type of wide range early screening test.

**Materials and Methods**

A method for extracting oral epithelial tissue was developed after IRB approval was requested and granted to work with human test subjects. All test subjects were presented with the same tissue extraction protocol after signing consent agreements.

Subjects were given 5 ml of distilled water and instructed to gently swish for 30 seconds to cleanse the mouth of unwanted particulate and mucosal matter. The rinse water was discarded. After a 5 minute waiting period following the first rinse, subjects were given 15 ml of distilled water and instructed to swish vigorously (with the intensity of a standard mouthwash rinse) for 90 seconds.

Subjects were then asked to spit the rinse water into a centrifuge tube. The rinse water was then poured through a cell strainer with a pore size of 100 um to eliminate mucous and obtain the cell extract.

The extract was then centrifuged at 130 rcf for 5 minutes and washed with phosphate buffered saline (PBS). The extract was centrifuged again at 200 rcf for 5 minutes and washed with PBS. The extract was then centrifuged at the same settings before being placed in a solution of 1% Bovine Serum Albumin (BSA) in PBS for 5 minutes. The extract was then centrifuged again at the same settings. 50 ul of .01% proflavine in PBS was then added to the pellet. 10 ul of the new solution was used to create one slide for imaging.

SCC-25, CAL-27, FaDu, and NCI-H1650 cancer cell lines were each grown separately with Dulbecco's Modified Eagle's Medium for SCC-25 and CAL-27 cells, Eagle's Minimum

Essential Medium for FaDu cells, and RPMI-1640 Medium for NCI cells. All media was mixed with additives to achieve a concentration of 10% Fetal Bovine Serum (FBS) and 1% penicillin streptomycin (penstrep).  All cells were incubated at 37 degrees C and 5% $CO_2$ until confluent, where confluent is defined as a stable monolayer of cells on a flask wherein a marked reduction in the speed of cell proliferation occurs. Cells were passaged and then subjected to the same collection process as the normal epithelial tissue.

SCC-25 cells are an immortalized cell line cultured from the biopsy of a squamous cell carcinoma of the tongue in a 70 year old man [11]. Today, the SCC line is widely used for cytological testing of oral cancers. CAL-27 cells were originally derived from a poorly differentiated squamous cell tongue carcinoma in a 56 year old man in 1982 [12]. Since then, there has been some debate on the actual cell type, with some labs reporting findings that indicate the cell line may in fact be an adenosquamous carcinoma [13]. Fadu cells originate from a squamous cell carcinoma in the hypopharynx of a 56 year old man [14].

SCC-25, CAL-27, and FaDu cells were both chosen due to their epidermal growth factor receptor (EGFR) and human epidermal growth factor receptor 2 (HER2) protein expression levels. EGFR and HER2 tyrosine kinases are proteins that are important in ligand-signaling cellular pathways that regulate cell death [15]. Cancer cells typically show increased levels of these receptors, and as such, have increased uptake levels of nutrients needed for cell growth and proliferation. All three cell lines show relatively low expression of EGFR and HER2 compared to other cell lines, which is desirable when you wish to stain the nuclei directly with proflavine.

NCI cells originate from the lungs and are from a bronchoalveolar carcinoma. These cells were chosen to represent a separate tissue type and to act as a control of sorts for the other cancer cell lines.

All cells were imaged using a custom built LED epi-illuminated fluorescence microscope. An LED that emitted blue light at 455 nm full width at half max (FWHM) was used to excite proflavine, which acts as a fluorophore and emits green light at 515 nm. Emission light was recorded by a Point Grey Flea 3 black and white camera. Images were recorded using both Point Grey Fly Cap software and a custom LabVIEW user interface. The LabVIEW interface allowed for input changes in both exposure time and gain, as well as quick image saving to a designated source destination.

Two cell types were used to highlight phenotypic characteristics of cell structure using proflavine. Both extracted epithelial cells and SCC-25 were imaged at variable settings with a 40x oil objective to obtain images that highlighted their physical differences.

Four cell types were used to quantify these phenotypic characteristics. Extracted epithelial cells were used as a normal control group. NCI cells were used as the dysplastic control group. CAL-27 and FaDu cell lines were imaged for the basis of the quantifications. All of these images were obtained with a 40x open air objective. The change in objective was critical, as the goal of this system is to provide a low cost alternative screening test to regions without means for other tests, and the air objective significantly cuts down on cost. When gathering this set of images, standard exposure times and gain were used. An exposure time of 100 ms with no gain were selected as the standards, as these settings prevented saturation in most cases. Saturation occurs when emitted light from the fluorophore exceeds an intensity of 255 (8 bit scale). When saturation occurs, data from analysis may be misconstrued because the actual intensity of the light exceeds what the camera is capable of recording.

Images were analyzed to find the size and brightness of the nuclear and cytoplasmic compartments. The blank or dark space of each image that did not contain any cells was also

recorded and analyzed to obtain a value for the level of noise associated with each data set. Noise is a measure of random pixel values that are not associated with the sample, and different types of noise exist. By measuring the pixel value of the blank space, background noise can be corrected for in data processing.

Image J software was used to identify components for imaging and to obtain pixel counts and pixel values for each compartment.  Data for each component was then input into Microsoft Excel for data processing. A custom MATLAB program was created to perform texture analysis on the sample sets by calculating the entropy, 'a statistical measure of randomness that can be used to characterize the texture of an input image.' [16] Entropy in MATLAB is defined as follows:

$$Entropy = -summation(p.*log2(p)),$$

where p is an array that contains the histogram count from the function imhist that stores histogram data from a set of images in MATLAB. Entropy can be thought of as the difference in pixel value between any two adjacent pixels. A high entropy indicates randomness throughout the image, whilst a low entropy represents a more ordered image.

Statistical analyses were performed to determine if significant differences existed between cell types. Two-tailed t-tests were used to examine any correlation between cell lines.

**Results**

Proflavine worked as a fluorophore and binded preferentially to the nucleus of each cell type. In addition to the nucleus, proflavine attached to and emitted light from the endoplasmic

reticulum, the cell membrane, assorted organelles, rod-shaped bacteria (bacillus), and was

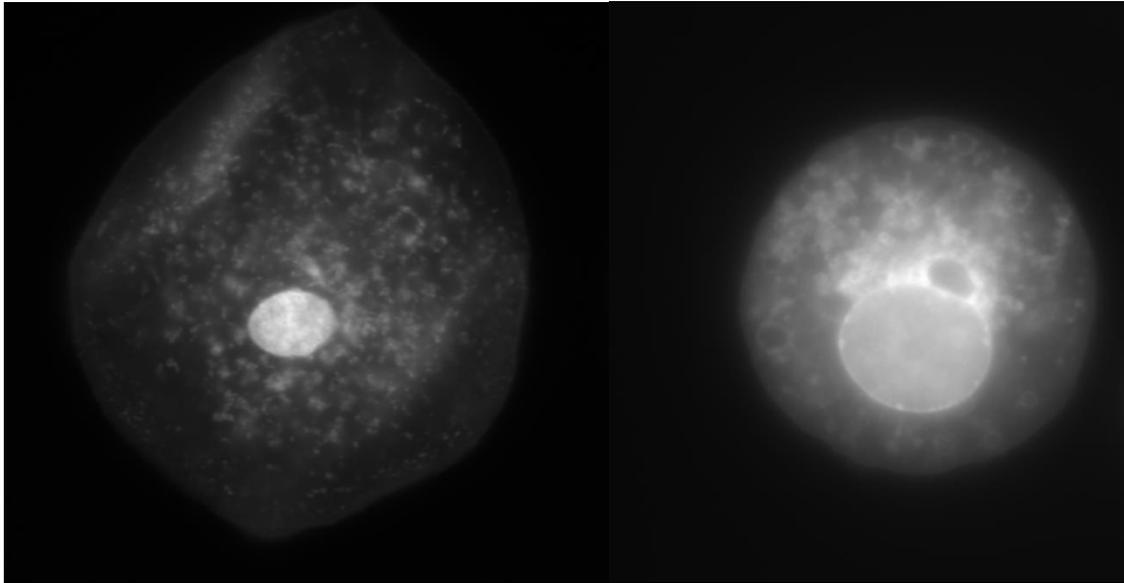present in high enough concentration to highlight the cytoplasm.



**Figure 1: (Left) Extracted normal epithelial cell showing clear differentiation between a bright nucleus and dark cytoplasm. Settings used were 38 ms exposure time and no gain. Image taken on 9-21-2013. (Right) CAL-27 OSCC showing nucleus, endoplasmic reticulum, and cytoplasm. Settings used were 19 ms exposure time and no gain. Image taken on 10-18-2013.**

The extraction process for normal oral epithelial cells went through several iterations

before becoming standardized. It was found that without a preliminary mouthwash, too much

mucous existed in the final extract product. The amount of mucous increased the difficulty of

cell extraction and reduced the total number of cells recovered. In addition, if any mucous was

still left in the extract at the imaging stage, it would prevent accurate results, as proflavine

becomes entrapped within the mucous and oversaturates the camera with the increased

concentration. Mucous amount was greatly reduced after the addition of a cell filter, which

increased both the ease of extraction and the reliability and validity of the quantification

processes.

The second change to the process was the concentration of proflavine used as an emission media. Originally, .1% proflavine was used in a solution of water. This resulted in a dark nuclei phenomenon, where many nuclei were as dark or darker than the background image. It also led to more radical changes in cell shape, as the cells were not accustomed to pure water. The concentration of proflavine was later changed to .01%, which provided the predictable results of a bright nuclei and relatively dark cytoplasm. When PBS was used as a buffer in place of water, cell shapes remained mostly static and similar to what would be expected. Figure 1 shows the difference the concentration of proflavine had on the appearance of the cell during imaging.
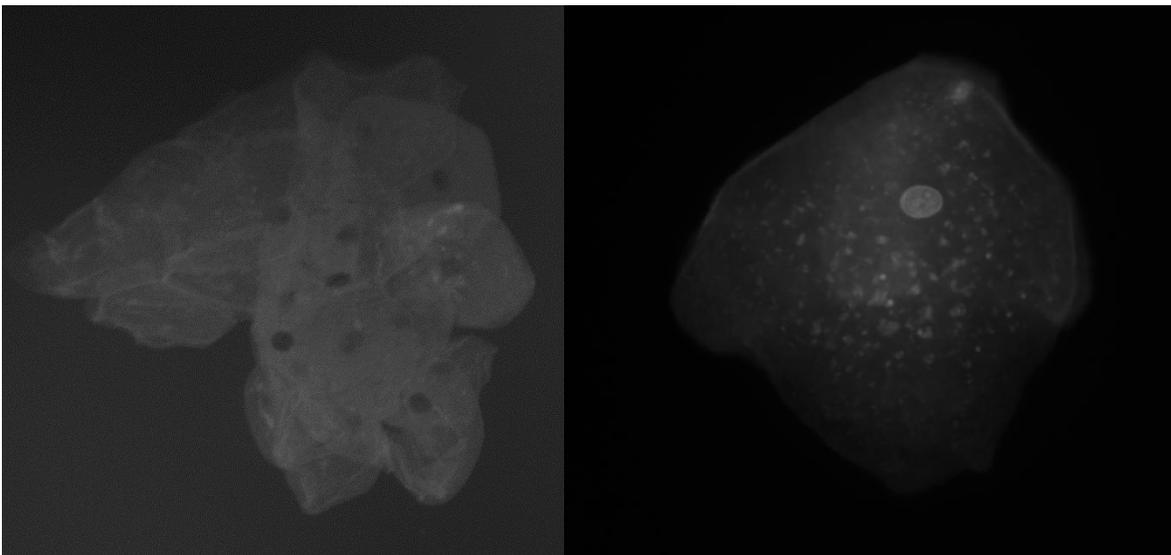


**Figure 2: (Left) Extracted normal epithelial cells from original trial run with .1% proflavine, no BSA, with a 10x are objective lens. Subjects commonly exhibited dark nuclei and excessive clumping. Settings used were 35 ms exposure time and 24 (max) gain (db). Image taken on 8-15-2013. (Right) Extracted normal epithelial cell after process refinement with .01% proflavine, BSA, with a 40x oil objective lens. Settings used were 147 ms exposure time and 997 gain. Image Taken on 9-10-2013.**

The use of BSA was another addition to the final process. When originally absent, cells tended to stick to one another. This invalidated many of the images for two main reasons: cells in clumps seemed to be preferentially targeted by proflavine and would typically be highly saturated, and cells would occasionally form a double or even triple layer, drastically altering the

pixel values in any given area. Two methods of applying BSA to the extract were tested. The first was to allow the cells to sit in BSA after being washed and before applying proflavine, and the second was a simple BSA wash. The wash provided minimal differences between standard and BSA applied groups, while allowing the cells to stay in BSA for five minutes provided a significant reduction in clumping in the final product.

The final iteration that was made to the extraction process involved the implementation of the proflavine. Originally, after adding proflavine to the extract, the cells would sit in the proflavine for five minutes before being placed in the centrifuge and then washed with PBS. This method provided bright images that did not experience rapid photobleaching; however, many of the cells imaged with this method became too bright and saturated the camera, resulting in a loss of validity. To correct this, proflavine was moved to the last step. The cells did not sit in proflavine, but instead were immediately imaged after the fluorophore's application. While this produced images that photobleached quicker and had slightly reduced overall brightness, it prevented most of the heavy saturation associated with the proflavine bath.

After the overall process had reached a point where results could be gathered reliably, cells were imaged at standardized settings and the different cellular components were quantified. Each had a distinct physical appearance, but there existed a much smaller difference between the less differentiated cancer lines.

Normal epithelial cells were characterized by a bright nucleus, semi-dark cytoplasm, and assorted bright organelles within the membrane. The average pixel value for the nucleus was $150.1 \pm 32.8$ and the average value for the cytoplasm was $68.5 \pm 19.5$. The average background noise was $6.5 \pm 4.1$. In normal epithial cells using the extraction process, nuclei were consistently over twice as bright as the surrounding cytoplasm.

CAL-27 OSCCs differed the most from other cell types. The average pixel value for the nucleus was $120.2 \pm 35.5$, while the average value for the cytoplasm was $70 \pm 39.8$. The average background noise was $3.7 \pm 1.6$. The average value for the cytoplasm did not see much of a change from the normal cells, but the nuclear brightness dropped significantly.

FaDu OSCCs had a similar range between nuclear and cytoplasm brightness when compared to normal and CAL-27 cells. The average pixel value of the nucleus was $188 \pm 18.4$, and the average pixel value of the cytoplasm was $126.9 \pm 27.4$. The average background noise for this cell line was $6.6 \pm 2.9$.

NCI cells showed a max brightness similar to the FaDu cell line, but had a much larger range between the nuclear and cytoplasmic compartments than the other cancerous cell lines. The average pixel value for the nucleus was $177.1 \pm 24.2$, while the average pixel value for the cytoplasm was $109.8 \pm 24.9$. The average background noise was $6.2 \pm 2.8$. These results are summarized in figure 4.

Next, the the size of both the nucleus and the total cell was analyzed. Since the value for cytoplasm area is simply the full cell area – nuclear area, cytoplasmic area is represented by the full area of the cell.  Normal epithelial cells had the smallest nuclear area and largest total area. The average nuclear area was $11478.5 \pm 3501.1$ pixels and the average total area was $543335 \pm 198932$ pixels.
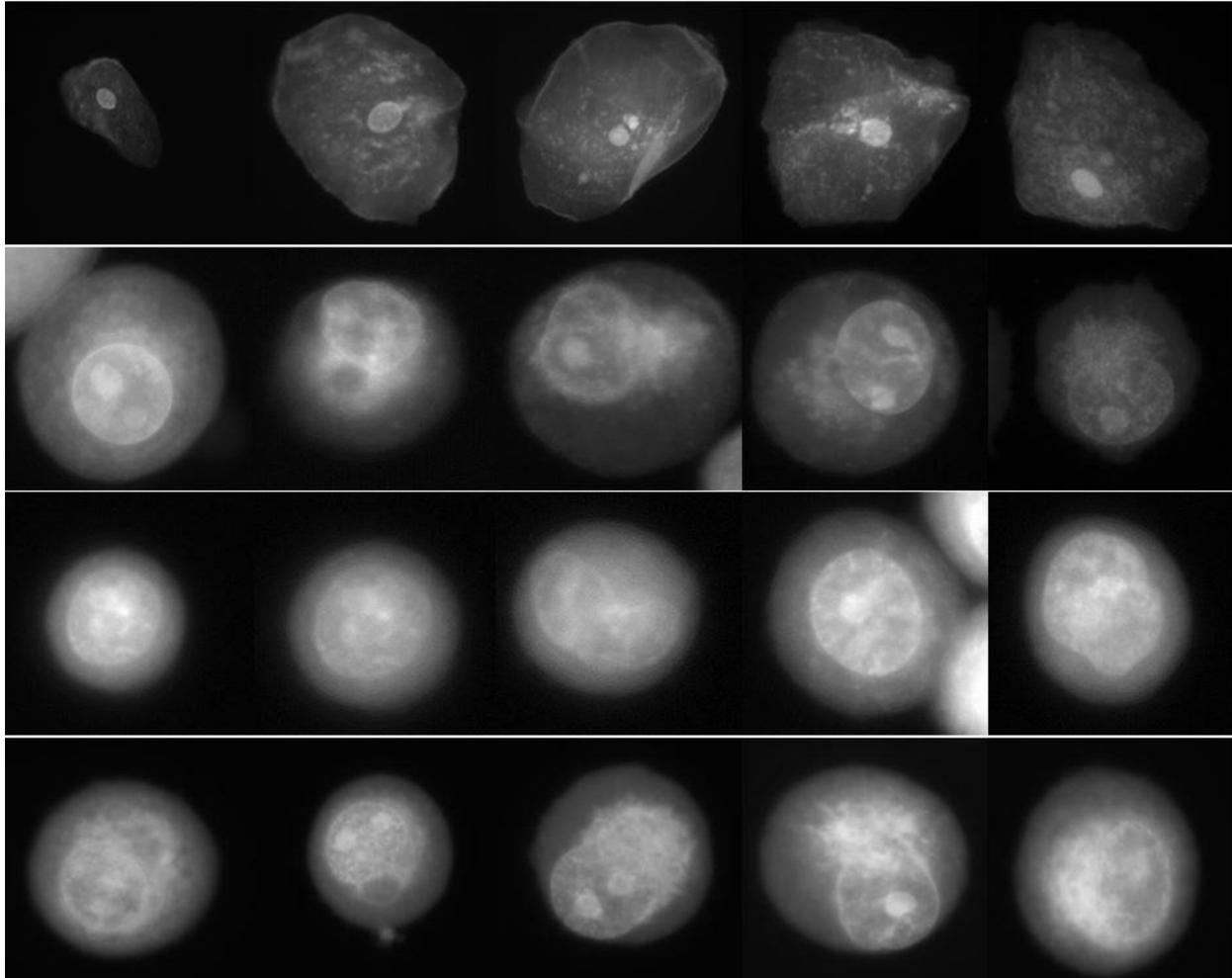
**Figure 3: (Top row) Extracted normal oral epithelial cells. (Second row) CAL-27 oral squamous carcinoma cells. (Third row). FaDu oral squamous carcinoma cells. (Bottom row) NCI lung cancer cells (image credit: Amy Powless). All images acquired using outlined process for cell imaging and taken at 100 ms exposure time with a 40x air objective lens.**

The average nuclear areas in the dysplastic cell lines were greater than in the normal epithelial cells, but on average, the area of the total cell was greatly reduced. CAL-27 cells had an average nuclear area of $22172.9 \pm 7732.7$ pixels. The average total cellular area of CAL-27 was $89614.4 \pm 43738.7$ pixels. This cell line had the largest total area and largest variability of total area of the tested dysplastic cell lines.

FaDu cells were the smallest cells in both nuclear and total cell areas. The average nuclear area was $16855.4 \pm 5182.21$ pixels an the average totl area was $43301.8 \pm 15628.7$ pixels.

NCI cells had the largest nuclear area of the dysplastic cell lines. The average nuclear area was $25293.1 \pm 10859$ pixels. The average total area was $88293 \pm 33361.6$ pixels. These results are summarized in figure 5.

Each cell lines raw data was then configured into ratios of nuclear data to cytoplasmic or total cell data. Pixel values associated with brightness were converted into a nuclear to cytoplasmic ratio, while pixel counts associated with area were converted into a nuclear to total cell ratio. This gave the percentage of total cell that the nucleus occupies.

Normal epithelial cells had the lowest size ratio and highest brightness ratio, with a size ratio of $.0211 \pm .01$ and a brightness ratio of $2.1905 \pm .787$.

CAL-27 cells had the next lowest size and second highest brightness ratios. The size ratio was $.2474 \pm .1484$, and the brightness ratio was $1.7157 \pm 1.096$.

FaDu cells had the highest size ratio and lowest brightness ratio. The size ratio was $.3893 \pm .1846$. The brightness ratio was $1.4814 \pm .352$. NCI cells had the second highest size ratio and second lowest brightness ratio. The size ratio was $.2865 \pm .164$. The brightness ratio was $1.6132 \pm .4278$. These results are summarized in figure 6.
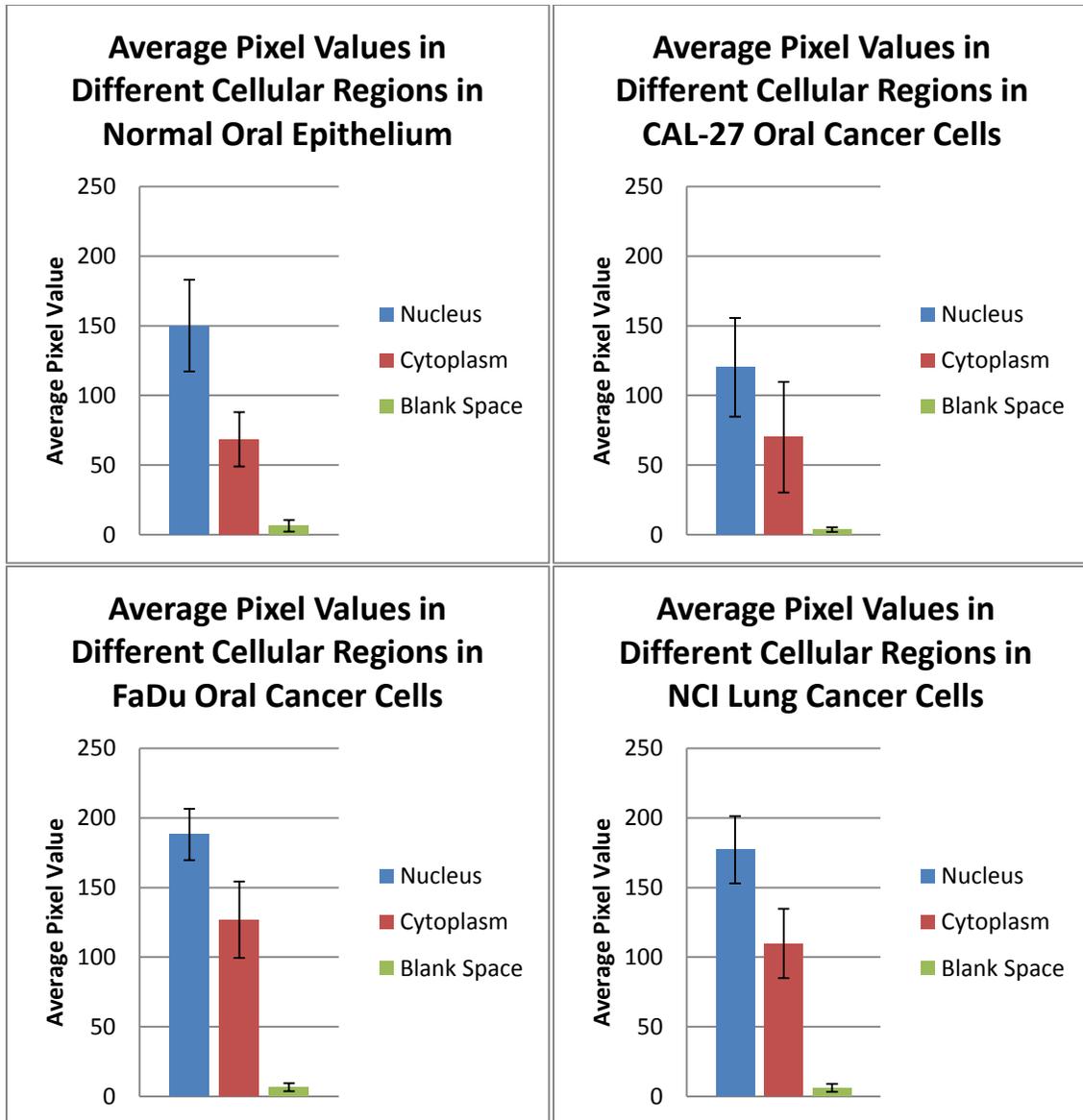
**Figure 4: (Top left)** Average pixel values of different cellular compartments in extracted normal epithelial cells. **(Top right)** Average pixel values of different cellular compartments in CAL-27 OSCCs. **(Bottom left)** Average pixel values of different cellular compartments in FaDu OSCCs. **(Bottom Right)** Average pixel values of different cellular compartments in NCI lung cancer cells. N = 50 for all data sets.

To test if a correlation existed between the relative sizes of the cell and the relative brightness of different compartments, the ratios were plotted against one another. For normal and nci cells, no distinct correlation existed between the two ratios. In FaDu cells, there existed a

slight positive trend, whereby increasing the ratio of nuclear to cell area increased the relative

brightness of the nucleus. In CAL-27 cells, a negative correlation existed between the two

 values. Increasing nuclear size decreased the nucear brightness. Figure 7 summarizes these
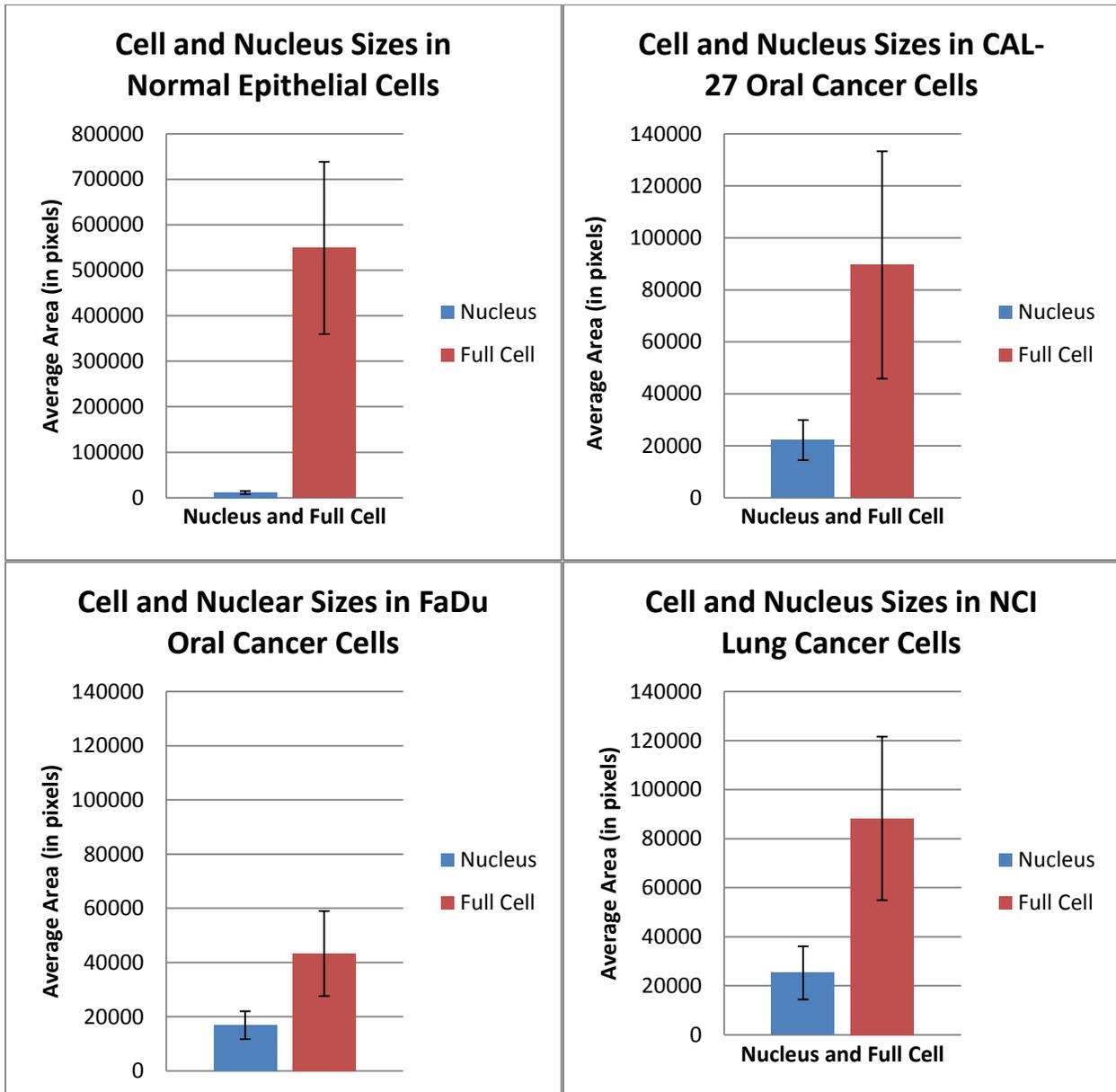
relationships.



**Figure 5: (Top left) Extracted normal epithelial cell total area and nuclear area. (Top right) CAL-27 OSCC total area and nuclear area. (Bottom left) FaDu OSCC total area and nuclear area. (Bottom right) NCI cell total area and extracted area. N=50 for all data sets.**
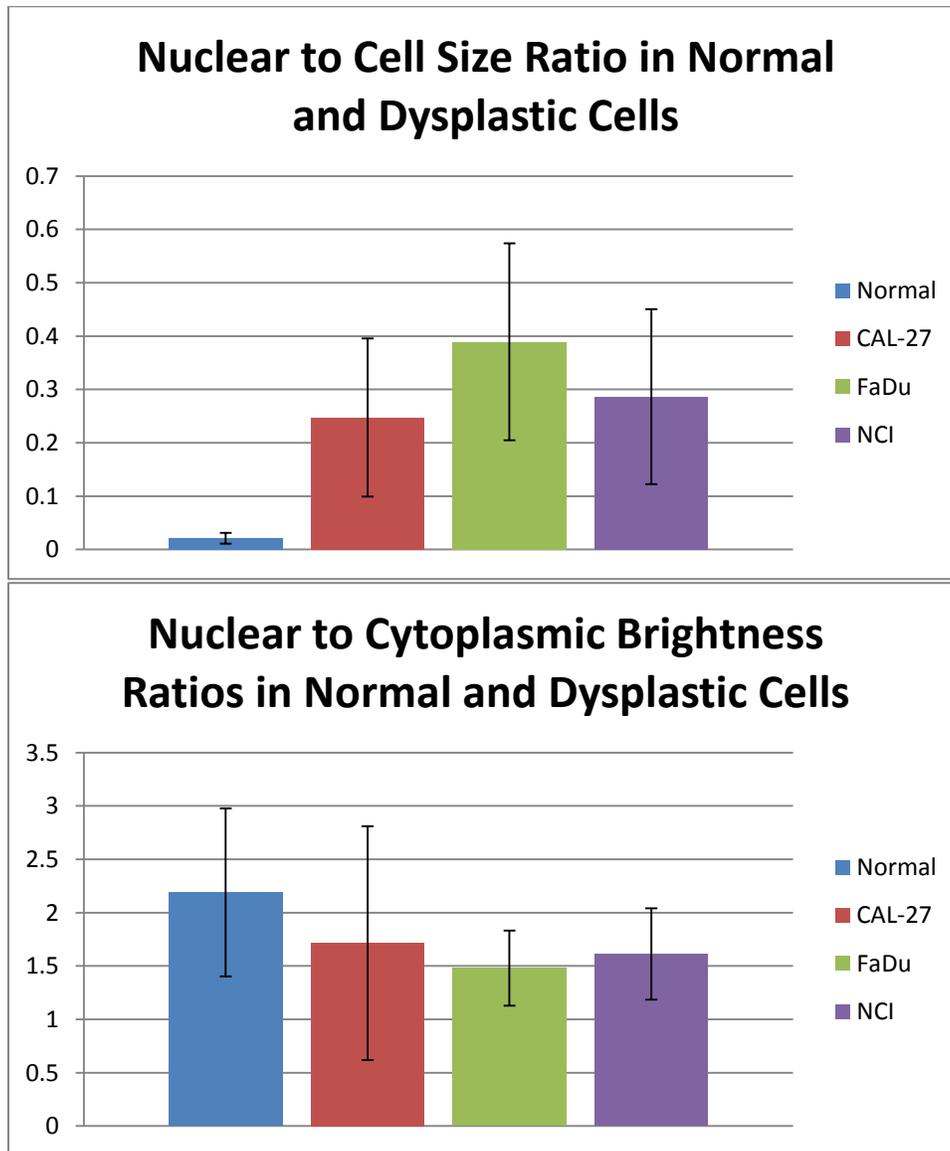
**Figure 6: (Top) Nuclear to total area ratio in the four quantified cell types: normal epithelial cells, CAL-27 OSCCs, FaDu OSCCs, and NCI lung cancer cells. (Bottom) Pixel value ratio between the nucleus and cytoplasm in the four quantified cell types. N=50 for both data sets.**
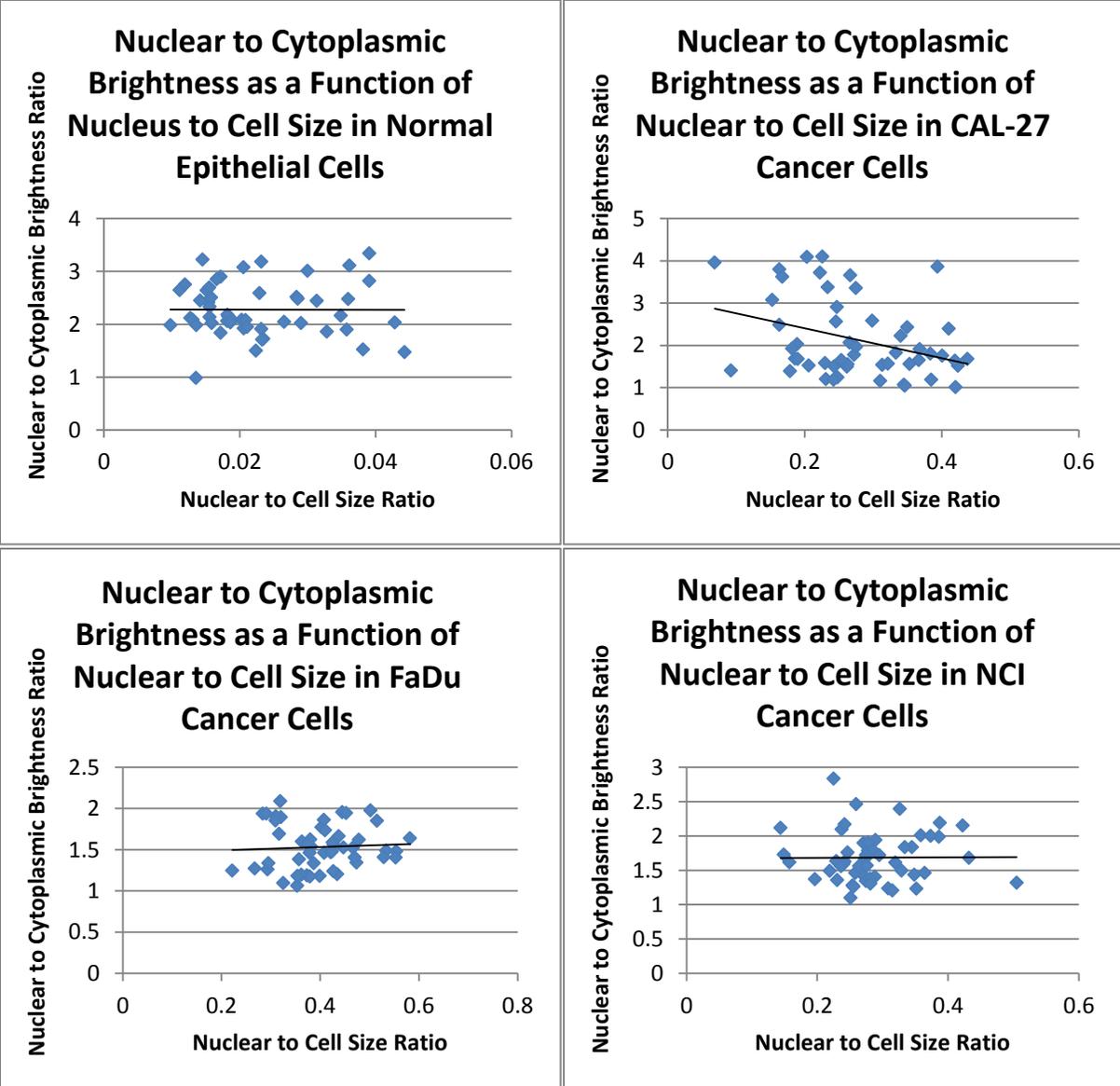
**Figure 7: Nuclear to Cytoplasmic Ratios compared against each other in selected cell types.**

Figure 8 shows the results from the MATLAB entropy analysis. Normal cells have a relaively high entropy compared to the dysplastic cell types, whose entropies are statistically similar. The entropy for normal cells was 4.5960. The entropy for CAL-27 cells was 3.6792. The entropy for FaDu cells was 3.7593. The entropy for NCI cells was 3.6109.
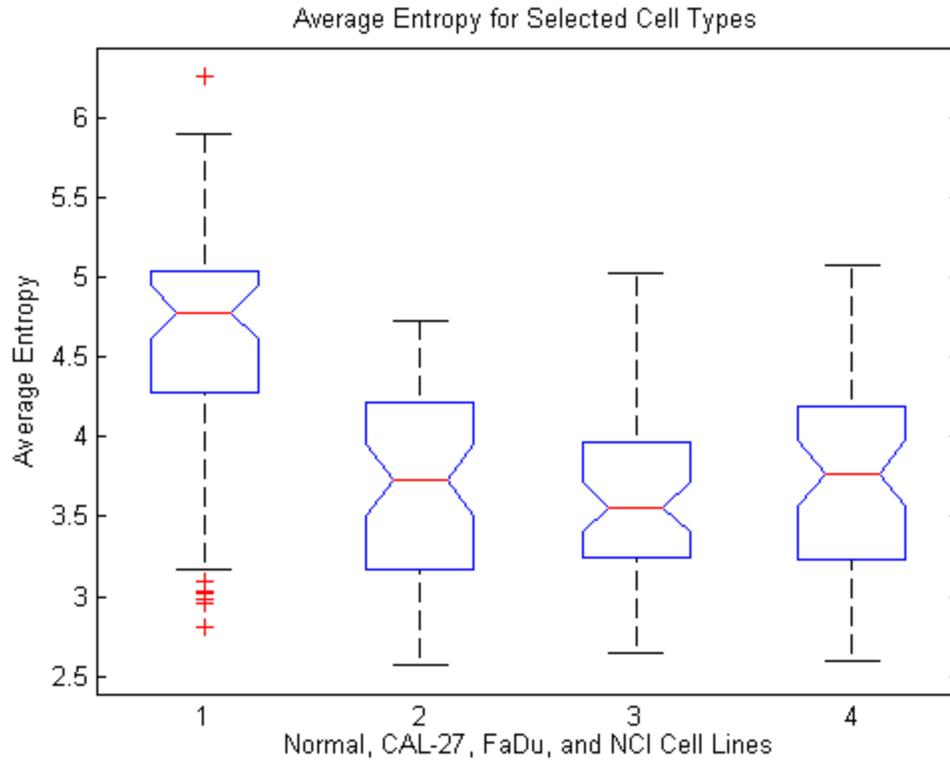
Figure 8: Entropy for selected cell types using a custom MATLAB code provided by Sandra Prieto. Normal oral cells had a higher average entropy than dysplastic cell lines. The red bar indicates the mean of the data, while the notches indicate the range of a 95% confidence interval. The range of the data is represented by the long bars, and statistical outliers are labelled with red plus signs. N=50 for all cell types.

T-tests comparing the nuclear and cytoplasm brightness and size were performed in excel and the results of these are found in figure 9.

| | Normal to CAL27 | Normal to FaDu | Normal to NCI | CAL27 to FaDu | CAL27 to NCI | FaDu to NCI |
|---|---|---|---|---|---|---|
| **Nucleus Brightness** | 2.56228E-05 | 2.05455E-10 | 2.66273E-05 | 3.66453E-21 | 6.60421E-15 | 0.007591815 |
| **Cytoplasm Brightness** | 0.777745985 | 1.2283E-21 | 4.13579E-14 | 4.34788E-13 | 6.88582E-08 | 0.000888325 |
| | | | | | | |
| **Nuclear Size** | 2.75804E-14 | 2.04879E-08 | 1.27554E-13 | 0.000136829 | 0.094852821 | 3.59307E-06 |
| **Full Size** | 3.48578E-31 | 3.90115E-34 | 1.64854E-31 | 3.16215E-10 | 0.992649284 | 7.16883E-14 |

Figure 9: T-tests between cell types for different nuclear and cytoplasmic values with reported p values. FaDu and NCI cells showed the most significant difference from normal oral cells in all areas examined.

**Discussion**

The finding of this project is that proflavine could be used as a cost effective fluorophore that would preferentially highlight the nucleus cells, but also could be used to view structures in the cytoplasm. It can be used in a manner similar to toluidine blue, but can only be applied in benchtop or cytological assays, as it is not approved for use in humans; however, this paper presents a method by which this cell by cell approach could be used in a clinical setting. By isolating a patients cells and using the outlined methods, one can differentiate between normal and dysplastic cells by their relative characteristics.

Cells differ in their base phenotypic characteristics depending on their location and function. Cancerous or dysplastic cells are less differentiated than normal epithelial cells, and present characteristics that are different than those found in normal cells. Specifically, the nucleus of cancer cells is larger than that of epithelial cells, to the point that it takes up a significant amount of space within the cell, to the point of being a third to a half of the total cell size. In contrast, the nuclei of normal oral epithelial cells is less than a tenth of the total cellular area. This could be because the cancer cells are metabolically active and always proliferating, and thus need a large deposit of RNA and DNA, and the normal epithelial cells are typically fully mature and have stopped dividing, and thus are no longer metabolically active.

This is supported by the brightness data obtained for FaDu and NCI cells. Both had significantly brighter nuclei than normal oral cells. Because proflavine intercalates between base pairs of DNA, it is expected that it would congregate in regions with high levels of DNA, and thus we would see higher pixel intensities in those regions during imaging. The low brightness data for CAL-27 cells could originate from improper handling of the cell line, which could have

led to early death for the cells, limiting their proflavine uptake. More testing is needed to confirm the results of each trial.

The brightness of the nuclei is also not due to cell size, as cells of different sizes consistently had randomly bright and dark nuclei.

Entropy data for each cell line suggests show that there is less variance between the pixel intensities over the entire range of dysplastic cells than over the entire range of normal epithelial cells. This is also supported by the nuclear to cytoplasmic brightness ratio, which is lower in dysplastic cells. This could mean that loose DNA or RNA exists in the cytoplasm of cancer cells, and it intercalates with the proflavine.

The data obtained during the course of this research could be used as the basis for the development of an index that catalogues the differences between normal and dysplastic epithelial cell types. Presented data that could be used in such an index are size, pixel intensity or brightness, texture, and nuclear to cytoplasmic ratios. These values have been shown to be sufficient to differentiate between normal and dysplastic cell types. Such an index would help those unfamiliar with the phenotypic characteristics of normal and dysplastic cells to differentiate between the two.

Using this index, we could transfer the manual analyzing of images to an automated process by constructing an algorithm that compares captured images to known values in the index. This algorithm could greatly cut down on both the time spent analyzing, and the level of knowledge and skill that would be needed to run the screening test, which fits within the goal of this project to create a cost effective screening tool that puts little to no strain on both the patient and investigator.

**Acknowledgements**

# References

1. Howlader N, Noone AM, Krapcho M, Garshell J, Neyman N, Altekruse SF, Kosary CL, Yu M, Ruhl J, Tatalovich Z, Cho H, Mariotto A, Lewis DR, Chen HS, Feuer EJ, Cronin KA (eds). SEER Cancer Statistics Review, 1975-2010, National Cancer Institute. Bethesda, MD, http://seer.cancer.gov/csr/1975_2010/, based on November 2012 SEER data submission, posted to the SEER web site, April 2013.

2. U.S. Cancer Statistics Working Group. *United States Cancer Statistics: 1999–2010 Incidence and Mortality Web-based Report*. Atlanta: U.S. Department of Health and Human Services, Centers for Disease Control and Prevention and National Cancer Institute; 2013. Available at: www.cdc.gov/uscs.

3. SEER Cancer Statistics Factsheets: Oral Cavity and Pharynx Cancer. National Cancer Institute. Bethesda, MD, http://seer.cancer.gov/statfacts/html/oralcav.html

4. Avon, S. Kliev, H. Oral Soft-Tissue Biopsy: An Overview. J Can Dent Assoc 2012;78:c75

5. Remmerbach, T. Weidenbach, H. Pomjanksi, N. Knops, K. Mathes, S. Hemprich, A. Bocking, A. Cytologic and DNA-cytometric early diagnosis of oral cancer. 2001. Analytical Cellular Pathology. 22:211-221.

6. Allegra E. Lombardo N. Puzzo L. Garozzo A. The usefulness of toluidine staining as a diagnostic tool for precancerous and cancerous oropharyngeal and oral cavity lesions. Acta Otorhinolaryngologica Italica. 2009;29:187-190

7. L. R. Ferguson, and W. A. Denny, "The genetic toxicology of acridines," Mutat. Res. 258(2), 123–160 (1991).

8. Sasikala, W. Mukherjee, A. Molecular Mechanism of Direct Proflavine-DNA Intercalation: Evidence for Drug-Induced Minimum Base-Stacking Penalty Pathway. The Journal of Physical Chemistry. 2012, 116 (40):12208-12212.

9. Prahl S. Proflavin. Oregon Medical Laser Center. http://omlc.ogi.edu/spectra/PhotochemCAD/html/078.html

10. Melhuish, W. H. (1964) Measurement of quantum efficiencies of fluorescence and phosphorescence and some suggested luminescence standards. J. Opt. Soc. Am. 54. 183-186.

11. Rheinwald J.; Becket M. Tumorigenic Keraticnocyte Lines Requiring Anchorage and Fibroblast Support Cultured from Human Squamous Cell Carcinomas. Cancer Research. 1981. 41:1657-1663

12. Gioanni J, Fischel JL, Lamber JC, Demard F, Mazeau C, Zanghellini E, Ettore F, Foremnto P, Chauvel P, Lalanne CM. Two new human tumor cell lines derived from squamous cell carcinomas of the tongue: establishment, characterization and response to cytotoxic treatment. European Journal of Cancer and Clinical Oncology. 1988 Sep;24(9):1445-55.

13. Lu Jiang, Ning Ji, Yu Zhou, Jing Li, Xianting Liu, Zhi Wang, Quanming Chem, Xin Zeng. Cal 27 is an oral adenosquamous carcinoma cell line. Oral Oncology. 2009. 45: e204-7.
14. Rangan, S. R. S. A new human cell line (FaDu) from a hypopharyngeal carcinoma. Cancer. 1972. 29:117-121
15. Rusnak, D.W.; Alligood, K.J.; Mullin, R.J.; Spehar, G.M.; Arenas-Elliott, C.; Martin, A.-M.; Degenhardt, Y.; Rudolph, S. K.; Jur Haws, T. F.; Hudson-Curtis, B.L.; Gilmer, T. M. Assessment of epidermanl growth factor receptor (EGFR, ErbB1) and HER2 (ErbB2) protein expression levels and response to lapatinib (Tkerb, GW572016) in an expanded panel of human normal and tumour cell lines. Cell Proliferation. 2007. 40(4):1365-2184
16. http://www.mathworks.com/help/images/ref/entropy.htm